

Article

Force-Based Characterization of the Wetting Properties of LDPE Surfaces Treated with CF₄ and H₂ Plasmas

Cihan Aktas¹ , Osman Polat¹ , Mohamadreza Beitollahpoor² , Melika Farzam² , Noshir S. Pesika² 
and Nurettin Sahiner^{1,3,4,*} 

¹ Department of Chemical, Biomolecular and Materials Engineering, University of South Florida, Tampa, FL 33620, USA

² Chemical and Biomolecular Engineering Department, Tulane University, New Orleans, LA 70118, USA

³ Department of Ophthalmology, Morsani College of Medicine, University of South Florida, 12901 Bruce B. Downs Blvd, MDC21, Tampa, FL 33612, USA

⁴ Department of Chemistry, Faculty of Science and Arts & Nanoscience, Technology Research and Application Center (NANORAC), Canakkale Onsekiz Mart University, Terzioğlu Campus, 17100 Canakkale, Turkey

* Correspondence: sahin71@gmail.com or nsahiner@usf.edu

Abstract: Low-density polyethylene (LDPE) films are widely used in packaging, insulation and many other commodity applications due to their excellent mechanical and chemical properties. However, the water-wetting and water-repellant properties of these films are insufficient for certain applications. In this study, bare LDPE and textured LDPE (T-LDPE) films were subjected to low-pressure plasmas, such as carbon tetrafluoride (CF₄) and hydrogen (H₂), to see the effect of plasma treatment on the wetting properties of LDPE films. In addition, the surface of the LDPE film was textured to improve the hydrophobicity through the lotus effect. The LDPE and T-LDPE films had contact angle (θ) values of $98.6^\circ \pm 0.6$ and $143.6^\circ \pm 1.0$, respectively. After CF₄ plasma treatments, the θ values of the surfaces increased for both surfaces, albeit within the standard deviation for the T-LDPE film. On the other hand, the contact angle values after H₂ plasma treatment decreased for both surfaces. The surface energy measurements supported the changes in the contact angle values: exposure to H₂ plasma decreased the contact angle, while exposure to CF₄ plasma increased the contact angle. Kinetic friction force measurements of water drops on LDPE and T-LDPE films showed a decrease in friction after the CF₄ plasma treatment, consistent with the contact angle and surface energy measurements. Notably, the kinetic friction force measurements proved to be more sensitive compared to the contact angle measurements in differentiating the wetting properties of the T-LDPE versus $3 \times$ CF₄-plasma-treated LDPE films. Based on Atomic Force Microscopy (AFM) images of the flat LDPE samples, the $3 \times$ CF₄ plasma treatment did not significantly change the surface morphology or roughness. However, in the case of the T-LDPE samples, Scanning Electron Microscopy (SEM) images showed noticeable morphological changes, which were more significant at sharp edges of the surface structures.

Keywords: LDPE; plasma modification; surface texture; wetting properties of LDPE; lotus effect



Citation: Aktas, C.; Polat, O.; Beitollahpoor, M.; Farzam, M.; Pesika, N.S.; Sahiner, N. Force-Based Characterization of the Wetting Properties of LDPE Surfaces Treated with CF₄ and H₂ Plasmas. *Polymers* **2023**, *15*, 2132. <https://doi.org/10.3390/polym15092132>

Academic Editors: Fahmi Zairi, Matthias Ballauff, Ulrich Maschke, Rufina G. Alamo and Martin Kröger

Received: 2 April 2023

Revised: 21 April 2023

Accepted: 27 April 2023

Published: 29 April 2023



Copyright: © 2023 by the authors. Licensee MDPI, Basel, Switzerland. This article is an open access article distributed under the terms and conditions of the Creative Commons Attribution (CC BY) license (<https://creativecommons.org/licenses/by/4.0/>).

1. Introduction

Polymers are crucial materials in various fields, such as packaging, adhesives, automotive and even the biomedical field [1]. Because of their inert nature and desired mechanical properties with tunable functional properties, polymers have replaced traditional engineering materials, such as metals and wood, and have been used in many forms and shapes, such as films, disk, plates, wire, foams, etc. [2,3]. Low-density polyethylene (LDPE) is one of the most widely used polymers in several industries, and its production is well established, easy and cheap [4,5]. Although LDPE has superior thermal, electrical and mechanical properties, it possesses a low surface free energy that affects its wettability and adhesion. LDPE similar to most of the commodity polymers are inert, and there are

several contamination layers on the surface, e.g., low-molecular-weight oligomers, additives, release agents, oil, etc. [6–8]. Those contaminations make the bonding on the surface of LDPE even more challenging [9]. Most of the industrial and biomedical applications require additional modifications of the polymer surfaces [9,10]. By changing the surface properties, it is possible to improve the wettability, printability and biocompatibility and, hence, enhance the applications of the polymers [11,12].

There are several methods available for the surface modifications of polymers. For example, Shenton et al. used atmospheric pressure plasma to increase the adhesive property of LDPE and polyethylene terephthalate (PET) [9]. Cheng et al. used the vapor phase deposition-initiated roll-to-roll method to modify cellulose chromatography paper [13]. Nejati et al. reported using lasers to functionalize the surface of carbon to attach silver nanoparticles on it [14]. Strobel and his coworkers exposed polypropylene (PP) to flames to improve its wettability [15]. Netravali and his colleagues used pulsed argon ion beams to increase the hydrophilicity of ultra-high-strength polyethylene fibers [16]. Further, even wet chemical techniques are available to functionalize the surface of crystals, such as gallium phosphide crystalline [17].

The low-pressure, cold plasma technique has many advantages for the surface modification of polymers [18–21]. Plasma treatment alters only a few tens to hundred angstroms of the samples' surface, while the bulk material remains unchanged [22]. Plasma gas treatment shows better homogeneity on surface modifications of polymers than corona discharge or flame exposure methods [18,23]. The treatments after the plasma process show better uniformity on the treated sample [24,25]. Furthermore, the exposure time can be kept noticeably short [26], and the parameters can be adjusted well and tuned with variable plasma gases and do not require any drying processes, such as wet chemical processes and solvent removal [27]. The plasma gas technique is ecological when the absence of chemical waste is considered [28]. Since it is a dry process, plasma treatment affords significant advantages for industrial applications.

In this study, commercially available LDPE and physically altered LDPE films (i.e., microtextured, as shown in Figure S1) were treated with CF_4 and H_2 plasmas. The plasma treatments were performed multiple times, e.g., up to three times, and the changes in the surface energy, water contact angle and roll-off angle were measured. The surface topography of textured LDPE (T-LDPE) samples was examined with the help of scanning electron microscopy (SEM, Hitachi 3400 electron microscope, Santa Clara, CA, USA), and the wetting properties of the surfaces were characterized by contact angle and sliding angle measurements, as well as by force-based friction measurements between a water drop and the films. This study shows the combined effects of the low-pressure plasma treatment and the surface texturing method on LDPE films.

2. Materials and Methods

2.1. Plasma Treatment

All the experiments for the capacitively coupled plasma gas treatments were conducted via a low-pressure radio frequency (RF, 13.56 MHz) plasma generator instrument (Femto AR-PC, Diener Electronic, Ebhausen, Germany). The low-pressure chamber of the plasma generator was evacuated by a rotary vane pump (16 m^3/h , Trivac D16BCS, Leybold Vakuum GmbH, Köln, Germany), and the pressure was monitored using a Pirani sensor. The inlet gas was introduced into the chamber at a flow rate of 1 mL/min by the mass flow controller of the plasma generator. The optimal working conditions of the plasma generator were set at 0.3 mbar, and the pressure was kept constant at that value during the plasma gas exposure. In the treatments of LDPE, H_2 and CF_4 gas plasmas were used. To dispose of the undesired gases from previous runs and the accumulated air from the waiting time, the plasma generator ran empty for 15 min prior to each plasma treatment. To determine the optimum parameters for the employed plasma gases, the LDPE samples were exposed to plasma gases for 2, 4, 6, 8, 10 and 15 min. For each time duration, the plasma power was varied as 30, 90 and 150 W values. After treatments, the water contact angles (CAs) were

measured via an optical tensiometer (Biolin Scientific, Attention Theta Flex, Phoenix, AZ, USA). A 150 W, 15 min exposure resulting in the highest CA value for the CF₄ treatment was chosen, whereas the lowest-CA-value resulting treatment from H₂ treatments was set with the optimum parameters of 30 W and 8 min.

To see the difference in single and multiple plasma gas treatments, samples were treated one time and three times with the same plasma gas. After treatments, the wetting properties, such as surface free energy, CA, sliding angle and water drop friction, were measured.

2.2. Surface Texturing of LDPE

Laser machining (CAJO, Technologies, New Orleans, LA, USA) was used to create a square lattice of circular holes (100 μm in diameter with 150 μm center-to-center spacing) on stainless steel. The latter served as a mold to create the textured LDPE films. In a typical molding step, the stainless-steel mold was preheated on a hotplate to 140 °C. A smooth LDPE film was placed on the mold and allowed to melt. Once the LDPE film turned translucent, a Teflon roller (McMaster-Carr, Douglasville, GA, USA) was used to compress the film so as to ensure that the liquid LDPE entered the holes in the stainless-steel mold. The latter was then cooled to room temperature, and the LDPE film was peeled off the surface, resulting in the textured LDPE film.

2.3. Measurements of Wetting Properties Using Contact Angles

The effect of functionalization via plasma treatment was assessed by the change in the wetting properties of the LDPE plate. The characterization of the plasma-treated samples' CA values was measured via an optical tensiometer. For the CA and surface free energy measurements, the sessile drop method was utilized. A 6 μL volume of liquid dropped on the surface of the sample was used, and 332 frames were recorded in 10 s.

In the sliding angle measurements, a volume of 100 μL distilled (DI) water was used. The sample holder was tilted at a rate of 90° per minute until the droplet slid off the sample surface. During the tilting, the droplets were captured at 5.5 frames per second (FPS), and the changes in CA on both sides of the drop were also recorded to measure the contact angle hysteresis (CAH). The CA, surface free energy and sliding angle CAH results were presented as the average of three different measurements. For the analysis of wetting properties, a software (One Attention from Biolin Scientific, Phoenix, AZ, USA, version 4.2.0) was used.

The OWRK (Owen, Wendt, Rabel and Kaelble) Model was utilized to evaluate the surface free energy of the polymer [29–32]. This model uses dispersive and polar force components of the material to calculate the surface free energy. The following equation, Equation (1), was used to determine the samples surface tensions.

$$\left(\gamma_{sv}^d \gamma_{lv}^d\right)^{\frac{1}{2}} + \left(\gamma_{sv}^p \gamma_{lv}^p\right)^{\frac{1}{2}} = 0.5 + \gamma_{lv}(1 + \cos(\theta_Y)) \quad (1)$$

where γ_{sv} and γ_{lv} are the surface tensions of the solids and liquids, respectively; superscripts "d" and "p" are the dispersive and polar force components; and, finally, θ_Y is the contact angle of the liquid. Previous studies show using water and diiodomethane produces the most accurate results [31,33]. For that reason, DI water and diiodomethane were used for the calculation of dispersive and polar force components.

2.4. Measurements of Wetting Properties using Force-Based Friction Measurements

A nanotribo-meter (UMT Multi-specimen Test system, Bruker (formally CETR), San Jose, CA, USA) with a sensitivity of ± 1 μN and a force range of ±10 mN was used to measure normal and lateral friction forces. The protocol developed by Beitollahpoor et al. [34] was followed. A total of 20 μL water drops were placed on a copper ring probe, with an inside diameter of 2.3 mm, and covered by a PDMS layer on the top so as to prevent each water drop from passing through the probe during compression of the drop on the

surfaces (Figure S2). In a typical run, the water drop held by the ring probe was brought into contact with the SH surface at the velocity of 2 mm/s. Once the drop touched the surface, a predetermined preload was applied on the drop for 20 s to allow the solid/liquid interface to equilibrate (resting time) within the static regime. In the next step, the ring probe began to move laterally, thereby sliding the drop on the surface under a constant load, at a velocity of 0.1 mm/s for 30 s. The feedback controller of the instruments ensured that the load was maintained at the desired value throughout this step. In the transition step, while the ring was moving, the water drop remained pinned on the SH surface, and the static friction increased. Typically, the highest friction force was obtained at the very moment the receding edge of the water drop began to slide, i.e., the static friction force, F_{\parallel}^{static} , or the threshold force. The transition regime was followed by the kinetic regime, in which the water drop slid while overcoming the dynamic friction force, $F_{\parallel}^{kinetic}$, on the SH surface. The drop was finally pulled off of the surface in the last step. Generally, if the surface is homogenous and void of defects, F_{\parallel}^{static} is greater than $F_{\parallel}^{kinetic}$. Each run was repeated at least five times, and the error bars correspond to the standard deviations.

3. Results

3.1. Contact Angle and Surface Free Energy Measurements

The effect of two different plasmas, CF_4 and H_2 , on the surface of LDPE was studied. For these two different LDPE surfaces, smooth and textured with microstructures were employed. Plasma treatment of the surfaces with either H_2 or CF_4 rendered the LDPE surfaces more hydrophilic or hydrophobic with respect to a virgin LDPE surface. The effect of multiple plasma treatments ($1\times$ or $3\times$) was also investigated to determine whether further modification after the first plasma treatments was possible.

The CA measurements were determined right after the plasma treatment of LDPE with CF_4 and H_2 plasma gases. Figure 1 shows the change in the CA of H_2 - and CF_4 -plasma-gas-treated samples.

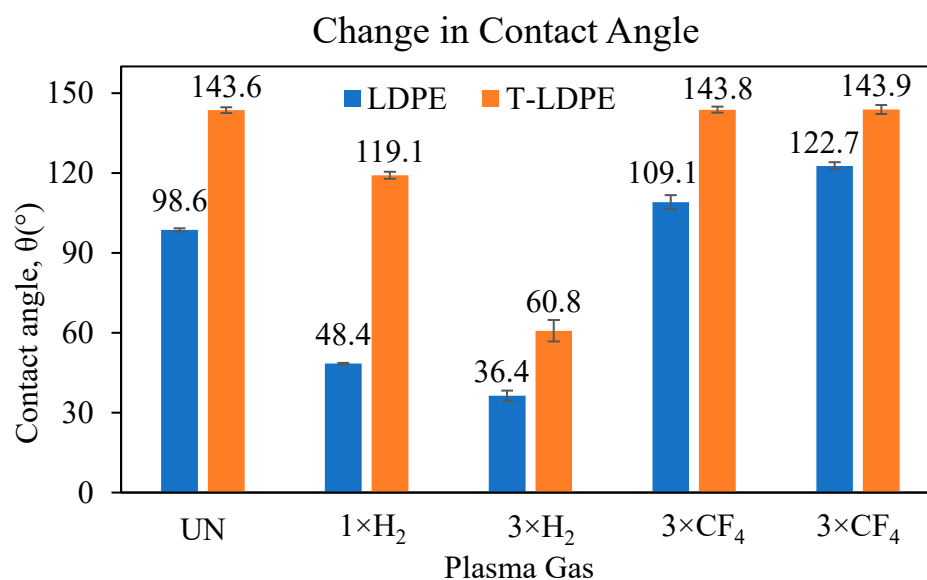


Figure 1. Contact angle (CA) values of LDPE and T-LDPE samples upon multiple H_2 and CF_4 plasma treatments.

After texturing the LDPE films, T-LDPE, the CA values increased drastically from $98.6^\circ \pm 0.6$ to $143.6^\circ \pm 1.0$. Since LDPE is inherently hydrophobic, the addition of surface roughness and texture is expected to increase the CA value. In this case, the surface texturing traps air pockets, and water drops remain in the Cassie–Baxter state [35]. After functionalization via CF_4 and H_2 plasma treatments, the wetting behavior of the smooth LDPE films showed a higher change than the T-LDPE samples. Upon H_2 plasma treatment,

the generation of radicals and species, such as H^+ , H_2^+ and H_3^+ , the functional groups on the surface of LDPE, reacts with air molecules and gases upon exposure to the atmospheric gases after the plasma treatment [36,37]. This can lead to the formation of more polar groups, such as double carbon bonds, hydroxyl, carboxyl, carbonyl, peroxide, ester and ether on the surface of the LDPE samples, which resulted in lower CA values, e.g., from $98.6^\circ \pm 0.6$ to $36.4^\circ \pm 2.0$ after the 3rd H_2 plasma treatment. This hydrophilicity is attributed to the increased interaction of the newly formed functional groups on the surface of LDPE with water molecules [38–40]. The T-LDPE samples followed a similar behavior, and their CA values changed from $143.6^\circ \pm 1.0$ to $60.80^\circ \pm 4.0$ after the 3rd H_2 plasma treatment. A reason for this could be the functionalization of additional surface groups after repeated H_2 plasma treatments. These results show that the chemical composition of the surfaces also plays a significant role in the surface wetting behavior, in addition to the surface morphology, emphasizing the availability of appropriate functional groups [41–43].

It was reported that the surface of the LDPE samples could be fluorinated upon CF_4 plasma treatment [41]. After introducing the C–CF, CF, CF_2 and CF_3 groups by means of CF_4 plasma treatments, the hydrophobicity of the materials increased [44–46]. The main reason for the increased hydrophobicity of fluorinated surfaces is the lower-density packing of fluorocarbons on those surfaces, which causes weaker van der Waals interactions with water [47]. Upon three consecutive CF_4 plasma treatments, the contact angle values for LDPE samples increased from $98.6^\circ \pm 0.6$ up to $122.7^\circ \pm 1.4$. On the other hand, the hydrophobicity of T-LDPE samples did not change significantly, as it was found to change $143.6^\circ \pm 1.0$ to $143.9^\circ \pm 1.6$ after the 3rd CF_4 plasma treatment. These results indicate that the polar force component of T-LDPE samples was almost unchanged after the CF_4 plasma treatment. The surface area of the T-LDPE in contact with the DI water droplet was much smaller in the Cassie–Baxter state in comparison to the LDPE with smooth surfaces, hence the adhesive forces, and this could be a reason for the unchanged contact angle values. Since the CA measurements were not sufficiently sensitive to detect changes in the wetting properties of the T-LDPE samples before and after CF_4 plasma treatment, a force-based measurement developed by Beitollahpoor et al. [34] was used and is presented in Section 3.3.

The surface free energies of the samples were also measured. Figure 2 depicts the changes of the surface free energies of LDPE samples after plasma treatments.

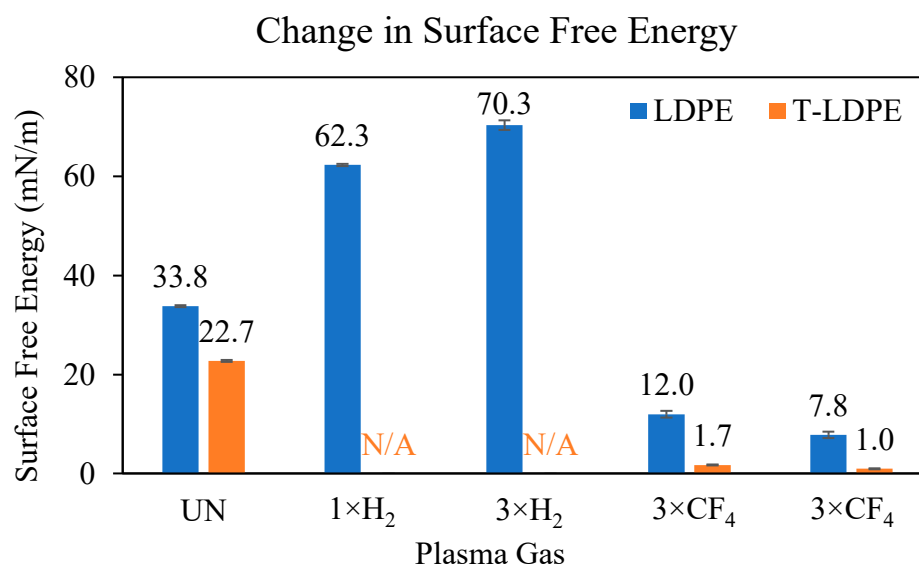


Figure 2. Change in surface free energies of LDPE samples and T-LDPE samples.

Since the measurements were determined with DI water and diiodomethane, the surface energy measurements can provide insight not only into the change in the polar force component, but also the change in the dispersive force component of the plasma-

treated LDPE and T-LDPE samples. The CA measurements resulted in an increase in hydrophilicity after H₂ plasma treatments for LDPE and T-LDPE. Therefore, the increase in the surface free energies was expected after H₂ plasma treatments. The surface free energy of LDPE increased from 33.8 ± 0.2 mN/m to 70.3 ± 1.0 mN/m after the 3rd H₂ plasma treatment. Unfortunately, the diiodomethane drops formed unmeasurable shapes on the surface of T-LDPE samples after H₂ plasma treatments; therefore, the surface free energy of these samples could not be measured.

CF₄ plasma treatments of both the LDPE and T-LDPE samples showed a decrease in surface free energies. These results were expected for LDPE samples, since the fluorination increased the hydrophobicity of the surface of the LDPE samples. The surface free energies of LDPE samples dropped from 33.8 ± 0.2 mN/m to 7.8 ± 0.7 mN/m after being treated 3 times with CF₄ plasma. Similarly, T-LDPE samples also dropped from 22.7 ± 0.2 mN/m to 1.0 ± 0.1 mN/m after the 3rd CF₄ plasma treatment. The surface free energy measurements show that the attraction from dispersive force component of both LDPE and T-LDPE surfaces decreased after the CF₄ plasma treatments.

3.2. Sliding Angle Measurements

Any chemical modifications on the sample surface also affects the necessary incline in the tilting angle to slide the droplets off the surface of LDPE and T-LDPE films. The tilting angle of the stage is referred to as the cradle angle, θ_c . Besides the sliding angles, the contact angle hysteresis (CAH) was also measured. During the tilting of the stage, gravitational force cause deformation in the shape of the droplets. This deformation leads to two results: (1) an increase in CA on one side of the droplets, which is called the advancing contact angle, θ_a , and (2) a decrease in CA on the other side of the droplets, known as the receding contact angle, θ_r . The difference between the advancing and the receding contact angle is the CAH [32,48,49]. On hydrophobic surfaces, the sliding occurs at low θ_c values, and the deformation in the shape of the droplets is usually very low. When the CA of a surface results in a value greater than 150° , the surface is called super hydrophobic. The CAH values of super-hydrophobic surfaces are close to 0° . The CAH measurements are summarized in Table 1, along with the values of various angles: the sliding angle (α), advancing contact angle (θ_a) and receding contact angle (θ_r) for LDPE and T-LDPE films after plasma gas treatments.

Table 1. Change in sliding angle (α), advancing contact angle (θ_a), receding contact angle (θ_r) and contact angle hysteresis (CAH) after plasma treatment of LDPE and T-LDPE samples.

Sample	Sliding Angle, α ($^\circ$)	Advancing Contact Angle, θ_a ($^\circ$)	Receding Contact Angle, θ_r ($^\circ$)	Contact Angle Hysteresis, CAH = $\theta_a - \theta_r$ ($^\circ$)
LDPE	12.5 ± 0.4	102.0 ± 0.8	80.1 ± 2.7	21.9
T-LDPE	6.9 ± 0.3	130.2 ± 3.5	110.5 ± 4.8	19.7
LDPE, 3 \times H ₂	14.7 ± 1.9	47.6 ± 0.6	7.6 ± 0.5	40
T-LDPE, 3 \times H ₂	38.2 ± 2.5	107.1 ± 3.5	23.2 ± 3.8	83.9
LDPE, 3 \times CF ₄	27.2 ± 2.7	141.1 ± 1.0	81.1 ± 2.1	59.9
T-LDPE, 3 \times CF ₄	1.7 ± 0.1	121.2 ± 0.7	118.3 ± 0.9	2.8

H₂-plasma-treated LDPE and T-LDPE samples show higher CAH values because of increased hydrophilicity. The sliding angle (α) for H₂-treated LDPE samples increased from $12.5^\circ \pm 0.4$ to $14.7^\circ \pm 1.9$. However, H₂ plasma treatment resulted in a much greater increase for T-LDPE samples. The surface roughness of T-LDPE samples can affect the droplets' grip on the surface. That effect can increase the droplet resistance against sliding off the T-LDPE surface. For CF₄-treated samples, on the other hand, the sliding angles of LDPE samples increased from $12.5^\circ \pm 0.4$ to $27.2^\circ \pm 2.7$. One reason for that could be the increased nanoscale roughness with the plasma etching, which can lead to drop pinning [41,50,51]. The increased roughness can make the droplets less prone to slide off

the surface of LDPE samples. The T-LDPE samples show almost perfect super-hydrophobic behavior after three consecutive CF_4 plasma treatments. The sliding angle drops from $6.9^\circ \pm 0.3$ down to $1.7^\circ \pm 0.1$, and the deformation on droplets is very low when compared to the other samples.

3.3. Force-Based Friction Measurements on T-LDPE Surfaces

Figure 3a compares the $F_{\parallel}^{kinetic}$ between a water drop and four surfaces: unmodified smooth LDPE, $3 \times \text{CF}_4$ -treated smooth LDPE, unmodified T-LDPE and $3 \times \text{CF}_4$ -treated T-LDPE. The force-based measurement could not be performed on the H_2 plasma-treated samples because the samples were too hydrophilic. As a result of the strong interaction between the water drop and the surface, the ring drop holder was unable to drag the water drop (i.e., the water drop remained pinned on the surface until it detached from the ring drop holder). An applied load equal to the weight of the 20 μL drop (i.e., 200 μN) was maintained during the measurement. The effect of the CF_4 treatment was apparent on both smooth and T-LDPE surfaces. In the case of the smooth LDPE surface, the $F_{\parallel}^{kinetic}$ dropped from an average value of 102 μN to 81.3 μN after the CF_4 treatment. The drop was even more significant on the T-LDPE surface, starting at an average value of 14.4 μN and decreasing to 3.17 μN after the CF_4 treatment. As demonstrated previously, CA measurements did not show significant differences between the unmodified and CF_4 -plasma-treated T-LDPE samples, even after $3 \times$ treatments. Using the nanotribometer, loads ranging from 100 to 1000 μN were applied and maintained on 20 μL drops during shearing against the unmodified and CF_4 -plasma-treated T-LDPE samples. Figure 3b shows a plot of $F_{\parallel}^{kinetic}$ as a function of the applied preload on a water drop as it is sheared on the T-LDPE surfaces. Under the entire load range of 100–1000 μN , the $F_{\parallel}^{kinetic}$ on the unmodified T-LDPE (yellow dashed lines) was greater than the $F_{\parallel}^{kinetic}$ on the CF_4 -plasma-treated T-LDPE (blue dashed lines). The lower $F_{\parallel}^{kinetic}$ on the CF_4 -plasma-treated T-LDPE is attributed to the lower surface energy provided by the CF_4 modification (See Figure 2). The water drop remained in the Cassie–Baxter state for both surfaces over the entire applied load range (i.e., the drop did not enter the Wenzel state).

3.4. SEM and AFM Images of Altered LDPE Samples

To see the effect of plasma treatment on surface morphology and roughness, AFM (Bruker Dimension ICON, San Jose, CA, USA) images of the $3 \times \text{CF}_4$ -plasma-treated flat LDPE were acquired, and the corresponding images are shown in Figure S3. As can be seen from the AFM images, the surface roughness did not change significantly. However, the SEM images of the T-LDPE samples presented in Figure 4a show significant surface morphological changes, as presented in Figure 4b at the tips of the surface structures, i.e., developing sharp edges after $3 \times \text{CF}_4$ treatments. The plasma process only affects a few tens of nm, maybe up to 50 nm [52,53] of the surface layer of the polymers, depending on the nature of the polymers, such as the crystallinity, glass transition temperature, MW and the extent and the nature of the functional groups. Upon comparison of the SEM images of the T-LDPE samples before and after $3 \times \text{CF}_4$, there is some morphological change in the surface of the T-LDPE samples that occurred due to the $3 \times \text{CF}_4$ treatments.

The low-pressure plasma process plays a very limited role in the physical alteration of the T-LDPE, depending on the plasma parameters, such as exposure time, power, etc.; however, it is possible to induce some slight alteration in the surface morphology of T-LDPE with plasma exposure, while maintaining the main features. As plasma parameters, e.g., power, exposure time, etc., can be controlled, it is possible to find appropriate parameters that do not induce recognizable changes on the surface features of T-LDPE. However, it may be necessary to make chemical modifications on the surface of LDPE, e.g., generation of C-F groups so that the chemical modification is achieved, and this can somehow change the surface morphology. Moreover, etching could play an important role in the surface modification of T-LDPE samples [54–56].

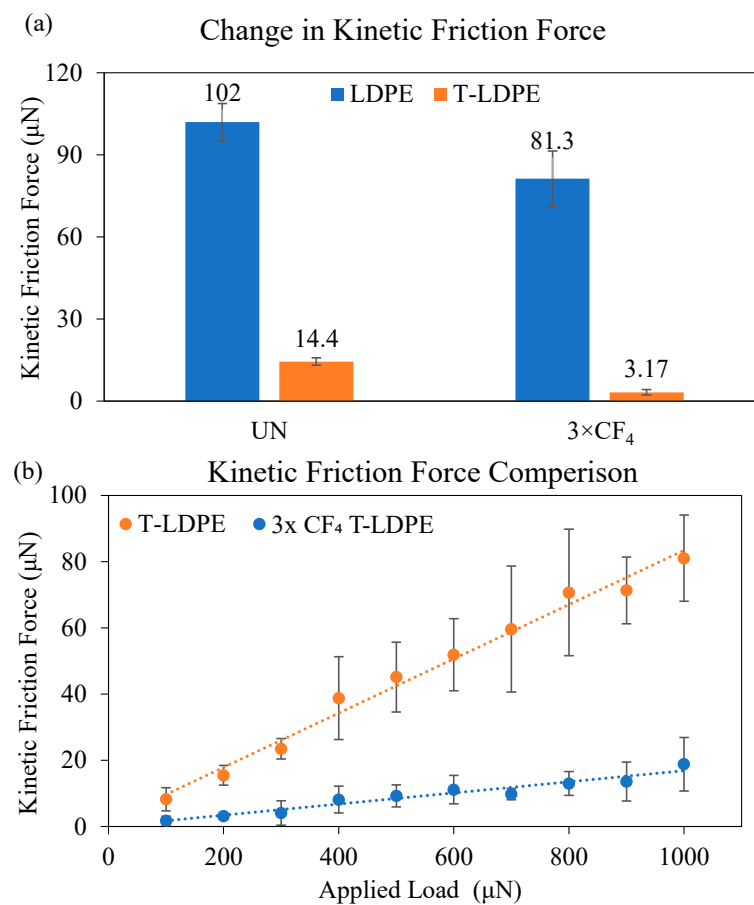


Figure 3. (a) Change in the $F_{\parallel}^{kinetic}$ of LDPE samples and T-LDPE samples after 3×CF₄ plasma treatment. The applied load on the water drop was maintained at 200 μN. (b) Plot of the $F_{\parallel}^{kinetic}$ versus applied normal load of a 20 μL water drop sheared against an unmodified (red data) and 3×CF₄-plasma-treated textured LPDE. The shear velocity is 0.1 mm/s. Each experiment was repeated at least 3 times, and error bars represent the standard deviations.

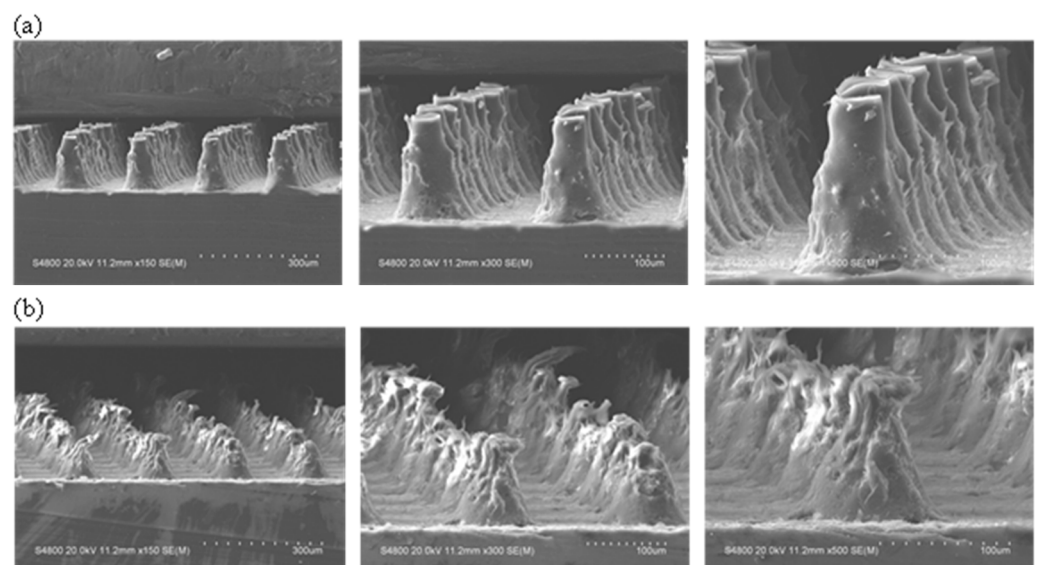


Figure 4. SEM images of (a) untreated T-LDPE and (b) after three times treatment with CF₄ (3×CF₄ T-LDPE) at 3 magnifications.

4. Conclusions

LDPE and T-LDPE samples were treated with successive H₂ and CF₄ plasmas. H₂ plasma treatments caused a decrease in water CA measurements, while CF₄ plasma treatments resulted in an increase in water CA measurements. After a 3rd H₂ plasma treatment, the surface free energy value of LDPE increased to 70.3 ± 1.0 mN/m from 33.8 ± 0.2 mN/m, and after a 3rd CF₄ treatment, the surface free energy value decreased to 7.8 ± 0.7 mN/m. The sliding angle α value of LDPE samples increased from $12.5^\circ \pm 0.4$ to $14.7^\circ \pm 1.9$ after the 3rd H₂ plasma treatment and to $27.2^\circ \pm 2.7$ after the 3rd CF₄ treatment. The CA of T-LDPE decreased from $143.6^\circ \pm 1.0$ to $60.8^\circ \pm 4.0$ after the 3rd H₂ plasma treatment and increased to $143.9^\circ \pm 1.6$ after the 3rd CF₄ plasma treatment. The surface free energy of T-LDPE decreased from 22.74 ± 0.2 mN/m to 1.0 ± 0.1 mN/m after the 3rd consecutive CF₄ plasma treatment. The sliding angle of T-LDPE samples increased to $38.2^\circ \pm 2.5$ from $6.9^\circ \pm 0.3$ after the 3rd H₂ plasma treatment and decreased to $1.7^\circ \pm 0.1$ after the 3rd CF₄ plasma treatment. The CAH values of the samples increased based on the increases of the hydrophilicity of the surfaces, regardless of the treatment. However, samples with surface features, e.g., T-LDPE, had a lower CAS than their non-textured surfaces, e.g., LDPE with smooth surfaces. After the 3rd consecutive CF₄ plasma treatment, the friction force between water drops, and LDPE and T-LDPE films dropped from 102 μ N to 81.3 μ N and from 14.4 μ N to 3.17 μ N, respectively. These results suggest that the combinatory effect of surface texturing and plasma gas treatments of LDPE provide significant changes in the wetting properties of surfaces, which are potentially advantageous in many applications using this material. The area of application of textured and plasma-treated samples not only include tubing, piping, packing and food and beverage, but also cover biomedical applications.

Supplementary Materials: The following supporting information can be downloaded at: <https://www.mdpi.com/article/10.3390/polym15092132/s1>, Figure S1: LDPE (top left) and T-LDPE (top right) samples. DI water forms different shapes on LDPE (bottom left) and on T-LDPE (bottom right); Figure S2: Optical image of the experimental setup used to measure the kinetic friction between a water drop and a textured LDPE sample. The water drop is 20 μ L. The copper ring drop holder is connected to a dual-axis force sensor which allows for simultaneous normal and lateral force measurements.; Figure S3: AFM images using tapping mode of flat LDPE samples (a) before, (b) after $3 \times$ CF₄ plasma treatment. The surface roughness (R_q) changes from 9.22 ± 3.73 nm to 10.28 ± 3.73 nm. The surface roughness values were obtained by averaging the roughness of 3 random locations on each sample.

Author Contributions: Conceptualization, N.S.P. and N.S.; methodology, C.A., O.P., M.B. and M.F.; software, N.S.P.; validation, C.A., N.S.P. and N.S.; formal analysis, N.S.P. and N.S.; investigation, C.A., O.P., M.B. and M.F.; resources, N.S.P. and N.S.; data curation, C.A., O.P., M.B. and M.F.; writing—original draft preparation, C.A., O.P., M.B. and M.F.; writing—review and editing, N.S.P. and N.S.; visualization, N.S.P. and N.S.; supervision, N.S.; project administration, N.S.; funding acquisition, N.S.P. and N.S. All authors have read and agreed to the published version of the manuscript.

Funding: Partial financial support from the startup fund (N. Sahiner) from Ophthalmology Department, Morsani College of Medicine at USF, is greatly appreciated. In addition, N. Pesika acknowledges support from the Louisiana Board of Regents and Intralox L.L.C. (LEQSF (2019-22)-RD-B-04).

Data Availability Statement: The data presented in this study are available on request from the corresponding author.

Acknowledgments: We also thank Roya Gadimli from the Albert group (Chemical and Biomolecular Engineering, Tulane, New Orleans, LA, USA) for the AFM imaging of samples.

Conflicts of Interest: The authors declare no conflict of interest.

References

1. Švorčík, V.; Kotál, V.; Slepíčka, P.; Bláhová, O.; Špírková, M.; Sajdl, P.; Hnatowicz, V. Modification of Surface Properties of Polyethylene by Ar Plasma Discharge. *Nucl. Instrum. Methods Phys. Res. B* **2006**, *244*, 365–372. [\[CrossRef\]](#)
2. Ataefard, M.; Moradian, S.; Mirabedini, M.; Ebrahimi, M.; Asiaban, S. Investigating the Effect of Power/Time in the Wettability of Ar and O₂ Gas Plasma-Treated Low-Density Polyethylene. *Prog. Org. Coat.* **2009**, *64*, 482–488. [\[CrossRef\]](#)
3. Sanchis, M.R.; Blanes, V.; Blanes, M.; Garcia, D.; Balart, R. Surface Modification of Low Density Polyethylene (LDPE) Film by Low Pressure O₂ Plasma Treatment. *Eur. Polym. J.* **2006**, *42*, 1558–1568. [\[CrossRef\]](#)
4. Olifirenko, A.S.; Novak, I.; Rozova, E.Y.; Saprykina, N.N.; Mitilineos, A.G.; Elyashevich, G.K. Hydrophilization of Porous Polyethylene Films by Cold Plasma of Different Types. *Polym. Sci. Ser. B* **2009**, *51*, 247–255. [\[CrossRef\]](#)
5. Drnovská, H.; Lapčík, L.; Buršíková, V.; Zemek, J.; Barros-Timmons, A.M. Surface Properties of Polyethylene after Low-Temperature Plasma Treatment. *Colloid. Polym. Sci.* **2003**, *281*, 1025–1033. [\[CrossRef\]](#)
6. Xie, T.; McAuley, K.B.; Hsu, J.C.C.; Bacon, D.W. Gas Phase Ethylene Polymerization: Production Processes, Polymer Properties, and Reactor Modeling. *Ind. Eng. Chem. Res.* **1994**, *33*, 449–479. [\[CrossRef\]](#)
7. Nowlin, T.E. Low Pressure Manufacture of Polyethylene. *Prog. Polym. Sci.* **1985**, *11*, 29–55. [\[CrossRef\]](#)
8. Dilks, A. Polymer Surfaces. *Anal. Chem.* **1981**, *53*, 802A–816A. [\[CrossRef\]](#)
9. Shenton, M.J.; Lovell-Hoare, M.C.; Stevens, G.C. Adhesion Enhancement of Polymer Surfaces by Atmospheric Plasma Treatment. *J. Phys. D Appl. Phys.* **2001**, *34*, 2754–2760. [\[CrossRef\]](#)
10. Patra, N.; Hladik, J.; Pavlatová, M.; Miličký, J.; Martinová, L. Investigation of Plasma-Induced Thermal, Structural and Wettability Changes on Low Density Polyethylene Powder. *Polym. Degrad. Stab.* **2013**, *98*, 1489–1494. [\[CrossRef\]](#)
11. Popelka, A.; Kronek, J.; Novák, I.; Kleinová, A.; Mičušík, M.; Špírková, M.; Omastová, M. Surface Modification of Low-Density Polyethylene with Poly(2-Ethyl-2-Oxazoline) Using a Low-Pressure Plasma Treatment. *Vacuum* **2014**, *100*, 53–56. [\[CrossRef\]](#)
12. Farzam, M.; Beitollahpoor, M.; Solomon, S.E.; Ashbaugh, H.S.; Pesika, N.S. Advances in the Fabrication and Characterization of Superhydrophobic Surfaces Inspired by the Lotus Leaf. *Biomimetics* **2022**, *7*, 196. [\[CrossRef\]](#) [\[PubMed\]](#)
13. Cheng, C.; Gupta, M. Roll-to-Roll Surface Modification of Cellulose Paper via Initiated Chemical Vapor Deposition. *Ind. Eng. Chem. Res.* **2018**, *57*, 11675–11680. [\[CrossRef\]](#)
14. Nejati, S.; Mirbagheri, S.A.; Waimin, J.; Grubb, M.E.; Peana, S.; Warsinger, D.M.; Rahimi, R. Laser Functionalization of Carbon Membranes for Effective Immobilization of Antimicrobial Silver Nanoparticles. *J. Environ. Chem. Eng.* **2020**, *8*, 104109. [\[CrossRef\]](#)
15. Strobel, M.; Branch, M.C.; Ulsh, M.; Kapaun, R.S.; Kirk, S.; Lyons, C.S. Flame Surface Modification of Polypropylene Film. *J. Adhes. Sci. Technol.* **1996**, *10*, 515–539. [\[CrossRef\]](#)
16. Netravali, A.N.; Caceres, J.M.; Thompson, M.O.; Renk, T.J. Surface Modification of Ultra-High Strength Polyethylene Fibers for Enhanced Adhesion to Epoxy Resins Using Intense Pulsed High-Power Ion Beam. *J. Adhes. Sci. Technol.* **1999**, *13*, 1331–1342. [\[CrossRef\]](#)
17. Mukherjee, J.; Peczonczyk, S.; Maldonado, S. Wet Chemical Functionalization of III–V Semiconductor Surfaces: Alkylation of Gallium Phosphide Using a Grignard Reaction Sequence. *Langmuir* **2010**, *26*, 10890–10896. [\[CrossRef\]](#)
18. Liston, E.M.; Martinu, L.; Wertheimer, M.R. Plasma Surface Modification of Polymers for Improved Adhesion: A Critical Review. *J. Adhes. Sci. Technol.* **1993**, *7*, 1091–1127. [\[CrossRef\]](#)
19. Primc, G. Surface Modification of Polyamides by Gaseous Plasma—Review and Scientific Challenges. *Polymers* **2020**, *12*, 3020. [\[CrossRef\]](#)
20. Liu, Y.-X.; Zhang, Q.-Z.; Zhao, K.; Zhang, Y.-R.; Gao, F.; Song, Y.-H.; Wang, Y.-N. Fundamental Study towards a Better Understanding of Low Pressure Radio-Frequency Plasmas for Industrial Applications. *Chin. Phys. B* **2022**, *31*, 085202. [\[CrossRef\]](#)
21. Desmet, T.; Morent, R.; De Geyter, N.; Leys, C.; Schacht, E.; Dubruel, P. Nonthermal Plasma Technology as a Versatile Strategy for Polymeric Biomaterials Surface Modification: A Review. *Biomacromolecules* **2009**, *10*, 2351–2378. [\[CrossRef\]](#) [\[PubMed\]](#)
22. Chan, C.-M.; Ko, T.-M.; Hiraoka, H. Polymer Surface Modification by Plasmas and Photons. *Surf. Sci. Rep.* **1996**, *24*, 1–54. [\[CrossRef\]](#)
23. Friedrich, J.F.; Geng, S.; Unger, W.; Lippitz, A.; Erdmann, J.; Gorsler, H.-V.; Wöll, C.; Schertel, A.; Bierbaum, K. Plasma Functionalization and Reorientation of Macromolecules at Polymer Surfaces. *Surf. Coat. Technol.* **1995**, *74–75*, 664–669. [\[CrossRef\]](#)
24. Nuzzo, R.G.; Smolinsky, G. Preparation and Characterization of Functionalized Polyethylene Surfaces. *Macromolecules* **1984**, *17*, 1013–1019. [\[CrossRef\]](#)
25. Harth, K.; Hibt, H. Surface Modification of Polypropylene in Oxygen and Nitrogen Plasmas. *Surf. Coat. Technol.* **1993**, *59*, 350–355. [\[CrossRef\]](#)
26. Mühlhan, C.; Weidner, S.; Friedrich, J.; Nowack, H. Improvement of Bonding Properties of Polypropylene by Low-Pressure Plasma Treatment. *Surf. Coat. Technol.* **1999**, *116–119*, 783–787. [\[CrossRef\]](#)
27. Bhowmik, S.; Bonin, H.W.; Bui, V.T.; Chaki, T.K. Physicochemical and Adhesion Characteristics of High-Density Polyethylene When Treated in a Low-Pressure Plasma under Different Electrodes. *J. Adhes.* **2006**, *82*, 1–18. [\[CrossRef\]](#)
28. Sanchis, R.; Fenollar, O.; García, D.; Sánchez, L.; Balart, R. Improved Adhesion of LDPE Films to Polyolefin Foams for Automotive Industry Using Low-Pressure Plasma. *Int. J. Adhes. Adhes.* **2008**, *28*, 445–451. [\[CrossRef\]](#)
29. Owens, D.K.; Wendt, R.C. Estimation of the Surface Free Energy of Polymers. *J. Appl. Polym. Sci.* **1969**, *13*, 1741–1747. [\[CrossRef\]](#)
30. Kaelble, D.H. Dispersion-Polar Surface Tension Properties of Organic Solids. *J. Adhes.* **1970**, *2*, 66–81. [\[CrossRef\]](#)

31. Yu, X.; Hörst, S.M.; He, C.; McGuiggan, P.; Kristiansen, K.; Zhang, X. Surface Energy of the Titan Aerosol Analog “Tholin.” *Astrophys. J.* **2020**, *905*, 88. [[CrossRef](#)]
32. de Gennes, P.G. Wetting: Statics and Dynamics. *Rev. Mod. Phys.* **1985**, *57*, 827–863. [[CrossRef](#)]
33. Hejda, F.; Solar, P.; Kousal, J. Surface Free Energy Determination by Contact Angle Measurements—A Comparison of Various Approaches. In Proceedings of the 19th Annual Conference of Doctoral Students, WDS’10 “Week of Doctoral Students 2010”, Charles University, Faculty of Mathematics and Physics, Prague, Czech Republic, 1–4 June 2010; Volume 19, pp. 25–30.
34. Beitollahpoor, M.; Farzam, M.; Pesika, N.S. Determination of the Sliding Angle of Water Drops on Surfaces from Friction Force Measurements. *Langmuir* **2022**, *38*, 2132–2136. [[CrossRef](#)] [[PubMed](#)]
35. Cassie, A.B.D.; Baxter, S. Wettability of Porous Surfaces. *Trans. Faraday Soc.* **1944**, *40*, 546. [[CrossRef](#)]
36. Lamichhane, P.; Acharya, T.R.; Kaushik, N.; Nguyen, L.N.; Lim, J.S.; Hessel, V.; Kaushik, N.K.; Choi, E.H. Non-Thermal Argon Plasma Jets of Various Lengths for Selective Reactive Oxygen and Nitrogen Species Production. *J. Environ. Chem. Eng.* **2022**, *10*, 107782. [[CrossRef](#)]
37. Sode, M.; Jacob, W.; Schwarz-Selinger, T.; Kersten, H. Measurement and Modeling of Neutral, Radical, and Ion Densities in H₂-N₂-Ar Plasmas. *J. Appl. Phys.* **2015**, *117*, 083303. [[CrossRef](#)]
38. Chu, P. Plasma-Surface Modification of Biomaterials. *Mater. Sci. Eng. R Rep.* **2002**, *36*, 143–206. [[CrossRef](#)]
39. Švorčík, V.; Kolářová, K.; Dvořánková, B.; Michálek, J.; Krumbholcová, E.; Hnatowicz, V. Plasma Modification of HEMA and EOEMA Surface Properties. *Radiat. Eff. Defects Solids* **2006**, *161*, 15–19. [[CrossRef](#)]
40. Švorčík, V.; Kolářová, K.; Slepíčka, P.; Macková, A.; Novotná, M.; Hnatowicz, V. Modification of Surface Properties of High and Low Density Polyethylene by Ar Plasma Discharge. *Polym. Degrad. Stab.* **2006**, *91*, 1219–1225. [[CrossRef](#)]
41. Polat, O.; Bhethanabotla, V.R.; Ayyala, R.S.; Sahiner, N. Carbon Tetrafluoride, Oxygen, and Air RF Plasma Modified Low-Density Polyethylene and Polydimethylsiloxane. *Plasma Chem. Plasma Process.* **2023**, *43*, 737–756. [[CrossRef](#)]
42. Gizer, S.G.; Bhethanabotla, V.R.; Ayyala, R.S.; Sahiner, N. Low-Pressure Plasma Treated Polycarbonate and Polymethyl Methacrylate (PMMA) Sheets with Different Surface Patterns to Change Their Surface Properties. *Surf. Interfaces* **2023**, *37*, 102646. [[CrossRef](#)]
43. Cordeiro, A.L.; Nitschke, M.; Janke, A.; Helbig, R.; D’Souza, F.; Donnelly, G.T.; Willemsen, P.R.; Werner, C. Fluorination of Poly(Dimethylsiloxane) Surfaces by Low Pressure CF₄ Plasma—Physicochemical and Antifouling Properties. *Express Polym. Lett.* **2009**, *3*, 70–83. [[CrossRef](#)]
44. Nitschke, M.; König, U.; Lappan, U.; Minko, S.; Simon, F.; Zschoche, S.; Werner, C. Low Pressure Plasma-Based Approaches to Fluorocarbon Polymer Surface Modification. *J. Appl. Polym. Sci.* **2007**, *103*, 100–109. [[CrossRef](#)]
45. Sawada, Y.; Kogama, M. Plasma-Polymerized Tetrafluoroethylene Coatings on Silica Particles by Atmospheric-Pressure Glow Discharge. *Powder Technol.* **1997**, *90*, 245–250. [[CrossRef](#)]
46. Zisman, W.A. Relation of the Equilibrium Contact Angle to Liquid and Solid Constitution. In *Contact Angle, Wettability, and Adhesion*; American Chemical Society: Washington, DC, USA, 1964; pp. 1–51.
47. Dalvi, V.H.; Rossky, P.J. Molecular Origins of Fluorocarbon Hydrophobicity. *Proc. Natl. Acad. Sci. USA* **2010**, *107*, 13603–13607. [[CrossRef](#)] [[PubMed](#)]
48. Dussan, V.E.B.; Chow, R.T.-P. On the Ability of Drops or Bubbles to Stick to Non-Horizontal Surfaces of Solids. *J. Fluid. Mech.* **1983**, *137*, 1–29. [[CrossRef](#)]
49. Joanny, J.F.; de Gennes, P.G. A Model for Contact Angle Hysteresis. *J. Chem. Phys.* **1984**, *81*, 552–562. [[CrossRef](#)]
50. Olde Riekerink, M.B.; Terlingen, J.G.A.; Engbers, G.H.M.; Feijen, J. Selective Etching of Semicrystalline Polymers: CF₄ Gas Plasma Treatment of Poly(Ethylene). *Langmuir* **1999**, *15*, 4847–4856. [[CrossRef](#)]
51. Acharya, T.R.; Chaudhary, D.K.; Gautam, S.; Singh, A.K.; Shrestha, R.; Adhikari, B.C.; Lamichhane, P.; Paudyal, B.; Kaushik, N.K.; Choi, E.H. Influence of Nanoparticle Size on the Characterization of ZnO Thin Films for Formaldehyde Sensing at Room Temperature. *Sens. Actuators A Phys.* **2023**, *351*, 114175. [[CrossRef](#)]
52. Nitschke, M.; Meichsner, J. Low-Pressure Plasma Polymer Modification from the FTIR Point of View. *J. Appl. Polym. Sci.* **1997**, *65*, 381–390. [[CrossRef](#)]
53. Grace, J.M.; Gerenser, L.J. Plasma Treatment of Polymers. *J. Dispers. Sci. Technol.* **2003**, *24*, 305–341. [[CrossRef](#)]
54. Liu, N.; Li, Z.; Chen, G.; Chen, Q.; Li, S. Space Charge Dynamics of CF₄ Fluorinated LDPE Samples from Different Fluorination Conditions and Their DC Conductivities. *Mater. Res. Express* **2017**, *4*, 075308. [[CrossRef](#)]
55. Egitto, F.D. Plasma Etching and Modification of Organic Polymers. *Pure Appl. Chem.* **1990**, *62*, 1699–1708. [[CrossRef](#)]
56. Riekerink, M.B.O. *Structural and Chemical Modification of Polymer Surfaces by Gas Plasma Etching*; Printpartners Ipskamp: Enschede, The Netherlands, 2001; ISBN 9789036516433.

Disclaimer/Publisher’s Note: The statements, opinions and data contained in all publications are solely those of the individual author(s) and contributor(s) and not of MDPI and/or the editor(s). MDPI and/or the editor(s) disclaim responsibility for any injury to people or property resulting from any ideas, methods, instructions or products referred to in the content.